Fluorescence Resonance Energy Transfer Biosensor Between Upconverting Nanoparticles and Palladium Nanoparticles for Ultrasensitive CEA Detection

Hui Li, Liang Shi, De-en Sun, Peiwu Li, Zhihong Liu

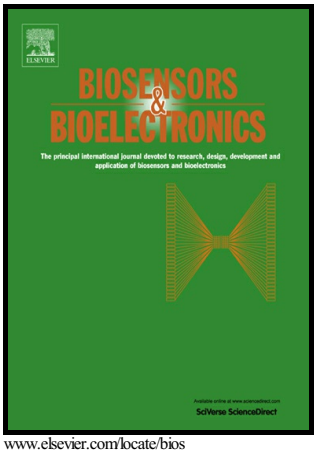

www.elsevier.com/locate/bios

PII: S0956-5663(16)30701-1
DOI: http://dx.doi.org/10.1016/j.bios.2016.07.070
Reference: BIOS8951

To appear in: *Biosensors and Bioelectronic*

Received date: 19 May 2016
Revised date: 19 July 2016
Accepted date: 21 July 2016

Cite this article as: Hui Li, Liang Shi, De-en Sun, Peiwu Li and Zhihong Liu Fluorescence Resonance Energy Transfer Biosensor Between Upconverting Nanoparticles and Palladium Nanoparticles for Ultrasensitive CEA Detection *Biosensors and Bioelectronic,* http://dx.doi.org/10.1016/j.bios.2016.07.070

Fluorescence Resonance Energy Transfer Biosensor Between Upconverting Nanoparticles and Palladium Nanoparticles for Ultrasensitive CEA Detection

Hui Li[a], Liang Shi[b], De-en Sun[c], Peiwu Li[a*], Zhihong Liu[c*]

[a]Oil Crops Research Institute of the Chinese Academy of Agricultural Sciences; Key Laboratory of Biology and Genetic Improvement of Oil Crops, Ministry of Agriculture; Key Laboratory of Detection for Mycotoxins, Ministry of Agriculture; Laboratory of Risk Assessment for Oilseeds Products (Wuhan), Ministry of Agriculture; Quality Inspection and Test Center for Oilseeds Products, Ministry of Agriculture, Wuhan 430062, PR China.

[b]Department of Pharmacy, Wuhan Children's Hospital, No. 100 Hongkong Rd, Wuhan 430016, PR China.

[c]Key Laboratory of Analytical Chemistry for Biology and Medicine (Ministry of Education), College of Chemistry and Molecular Sciences, Wuhan University, Wuhan 430072, PR China.

E-mail: peiwuli@oilcrops.cn

E-mail: zhhliu@whu.edu.cn

[*] Tel: 86-27-86812943; Fax: 86-27-86812862;

[*]Tel: 86-27-87217886; Fax: 86-27-68754067;

Abstract

An ultrasensitive biosensor for carcinoembryonic antigen (CEA) was constructed based on fluorescence resonance energy transfer (FRET) between upconverting nanoparticles (UCPs) and palladium nanoparticles (PdNPs). PdNPs was synthesized by the addition of a solution of Na_2PdCl_4 into a mixture of $N_2H_4 \cdot H_2O$ as the reducing agent and 11-mercaptoundecanoic acid

(MUDA) as the stabilizer. The CEA aptamer (5'-NH_2-ATACCAGCTTATTCAATT-3') was conjugated to hexanedioic acid (HDA) modified UCPs (HDA-UCPs) through an EDC-NHS coupling protocol. The coordination interaction between nitrogen functional groups of the CEA aptamer and PdNPs brought UCPs and PdNPs in close proximity, which resulted in the fluorescence quenching of UCPs to an extent of 85%. And the non-specific fluorescence quenching caused by PdNPs towards HDA-UCPs was negligible. After the introduction of CEA into the UCPs-CEA aptamer-PdNPs fluorescence quenching system, the CEA aptamer preferentially combined with CEA accompanied by the conformational change which weakened the coordination interaction between the CEA aptamer and PdNPs. So fluorescence recovery of UCPs was observed and a linear relationship between the fluorescence recovery of UCPs and the concentration of CEA was obtained in the range from 2 pg/mL to 100 pg/mL in the aqueous buffer with the detection limit of 0.8 pg/mL. The ultrasensitive detection of CEA was also realized in diluted human serum with a linear range from 4 pg/mL to 100 pg/mL and a detection limit of 1.7 pg/mL. This biosensor makes the most of the high quenching ability of PdNPs towards UCPs with negligible non-specific fluorescence quenching and has broad application prospects in biochemistry.

Keywords: Palladium Nanoparticles, Fluorescence Quenching Ability, Upconverting Nanoparticles, Carcinoembryonic Antigen, Fluorescence Resonance Energy Transfer

1. **Introduction**

It has been reported that 8.2 million deaths were caused by cancer in 2012 and the number continues to grow every year (Lee et al., 2015). Therefore it is very urgent to detect tumor

markers accurately and sensitively at the early stage of cancer and after treatment so as to provide sufficient information for clinical diagnosis and prognosis. Carcinoembryonic antigen (CEA) has been recognized as one of the most important tumor markers in lung, breast, gastrointestinal and ovarian cancer (Yang et al., 2015). Over the past few years several methods have been developed to detect the concentration of CEA, which include colorimetric immunoassay (Liu et al., 2014; Luo et al., 2015), enzyme-linked immunosorbent assay (ELISA) (EI-Masry et al., 2007; Urva et al., 2009), surface plasmon resonance based immunoassay (Ladd et al., 2009; Špringer et al., 2014), electrochemical immunoassay (Laboria et al., 2010; Martínez-Mancera et al., 2015), chemiluminescent immunoassay (Qu et al., 2013; Pal and Bhand, 2015), fluorescence immunoassay (Kim et al., 2014; Wu et al., 2015) and so on. Among all these methods, the homogeneous fluorescence assay based on FRET has attracted great attention because of its high sensitivity, ease of operation and time saving. However, traditional FRET donors mainly refer to down-conversion fluorophores such as organic dyes, which usually suffer from serious background interference including autofluorescence and scattering light when used in biological matrix under UV-visible light excitation. The emerging of upconverting nanoparticles (UCPs) admirably solves the above problems due to its near-infrared excitation and visible emission property. They have been widely used as FRET donor to construct biosensing platform for various biomolecules detection in complex matrix samples (Kuningas et al., 2005; Kuningas et al., 2006; Rantanen et al., 2008; Bogdan et al., 2010; Achatz et al., 2011; Wang et al., 2013; Li et al., 2014; Liu et al., 2014; Lv et al., 2015; Ma et al., 2015). The sensitivity of such biosensors also greatly depends on the fluorescence quenching ability of energy acceptors towards UCPs. Organic dyes are the commonly used energy acceptor in FRET biosensors but

their fluorescence quenching ability towards UCPs is not so satisfactory (Song et al., 2012). Recently many researchers focus on constructing FRET biosensors based on the excellent fluorescence quenching ability of carbon nanomaterials such as carbon nanoparticles, graphene and so on (Zhang et al., 2011; Wang et al., 2011; Wu et al., 2012; Zeng and Yuan et al., 2013). However, the non-specific adsorption caused by carbon nanomaterials greatly restricted its wide application in practical samples (Li et al., 2014). It has been reported that noble-metal nanoparticles including gold or silver nanoparticles could effectively quench the fluorescence of UCPs and hence sensitive biosensing platforms have been established accordingly (Wang et al., 2005; Wang et al., 2009; Xiao et al., 2015). The fluorescence quenching ability of PdNPs towards fluorescent dyes has been reported in a few studies (Kandela et al., 2007; Meyer et al., 2010). Li et al. also demonstrated that larger PdNPs (ca. 30 nm) exhibited broad and strong absorption in the whole UV-vis spectrum range and an ultrasensitive biosensor for DNA and protein detection was constructed based on the luminescence quenching ability of PdNPs towards fluorescence dyes accordingly (Li et al., 2015). What's more, the strong coordination interaction between hetero-atoms containing biomolecules such as DNA or peptide and PdNPs was also verified. Therefore we can safely infer that PdNPs may also be effectively used as fluorescence quencher for UCPs and a FRET biosensor for CEA detection based on the coordination interaction between CEA aptamer and PdNPs could be successfully developed.

CEA aptamer has been screened out by Hashemi Tabar et al. (Hashemi Tabar et al., 2010) and then different kinds of CEA aptasensors were constructed accordingly (Lin et al., 2012; Zeng and Ma et al., 2013; Zhou et al., 2014, 2015; Wang et al., 2015). In this paper, amino modified CEA aptamer was conjugated to hexanedioic acid (HDA) modified UCPs through an EDC-NHS

coupling protocol. The strong coordination between CEA aptamer and PdNPs greatly shortened the distance between UCPs and PdNPs into the range from 1 nm to 10 nm, and hence FRET between energy donor (UCPs) and acceptor (PdNPs) occurred accompanied by the observing of fluorescence quenching phenomenon of UCPs. After introducing CEA into the UCPs-CEA aptamer-PdNPs FRET quenching system, the conformational change of CEA aptamer binding with CEA largely weakened the coordination interaction between CEA aptamer and PdNPs, which inhibited the occurrence of FRET process. Fluorescence recovery of UCPs was observed and a linear relationship between the degree of fluorescence recovery and the concentration of CEA was obtained accordingly. The CEA biosensor also performed well in diluted human serum samples.

2. Materials and method

2.1 Materials

CEA, Bovine serum albumin (BSA) and immunoglobulin G (IgG) were obtained from Wuhan Boster Biological Technology Co., Ltd. Amine modified CEA aptamer (5'-NH_2-ATACCAGCT-TATTCAATT-3') was supplied by Sangon Biotechnology Co., Ltd (Shanghai, China). 2-(N-Morpholino) ethanesulfonic acid (MES), Tris(hydroxymethyl)aminomethane (Tris), N-Hydroxysuccinimide (NHS)，1-(3-dimethylaminopropyl)-3-ethylcarbodiimide hydrochloride (EDC·HCl) and 11-Mercaptoundecanoic acid (MUDA) were purchased from Sigma-Aldrich. N-(2-Hydroxyethyl) piperazine-N′-2-ethane sulfonic acid (HEPES) was from Alfa-Aesar. Fresh human serum samples were collected from healthy volunteers in Zhongnan Hospital, Wuhan University School of Medicine. The other reagents were all from Sinopharm Chemical Reagent Co., Ltd. (Shanghai, China). The solvents and reagents were used as received without further

purification. All aqueous solutions were prepared in ultrapure water (purified by Milli-Q biocel from Millipore China Ltd.).

2.2 Instrumentation

The crystalline phases of HDA coated $NaYF_4$:Yb,Tm upconverting nanoparticles and MUDA modified PdNPs were characterized by a Bruker D8 Discover X-ray diffractometer (XRD) with 2θ range from 10º to 70º at a scanning rate of 4º per minute, with Cu Ka irradiation (k = 1.5460 Å). The sizes and morphologies of HDA-UCPs and MUDA-PdNPs were analyzed by HITACHI H-7000FA transmission electron microscopy (100 kV accelerating voltage) and a JEM-2010 transmission electron microscopy (200 kV accelerating voltage). UV-vis absorption measurements were performed on a UV2550 UV-vis spectrophotometer (Shimadzu Scientific Instruments Inc.). The upconverting fluorescence spectra were measured on a RF5301 fluorescence spectrophotometer (Shimadzu Scientific Instruments Inc.) using a 980 nm diode continuous-wave (CW) laser (Beijing Hi-Tech Optoelectronic Co., Ltd.) as the external excitation source, the power of which was 850 mW.

2.3 Synthesis of Oleic Acid-modified $NaYF_4$: Yb, Tm Upconverting Nanoparticles

Oleic acid (OA)-modified $NaYF_4$: Yb, Tm upconverting nanoparticles were synthesized as reported by Cui et al. (Cui et al., 2011). Firstly, excess nitric acid was added into 0.6 mmol of lanthanide oxides Ln_2O_3 (Y:Yb:Tm =0.795:0.2:0.005 in mol) and the mixture was heated to 65 °C to dissolve Ln_2O_3, then the solvent was evaporated by heating to 145 °C for 6 h to obtain solid $Ln(NO_3)_3$. Subsequently, H_2O (5 mL), NaOH (1.2 g, 30 mmol), ethanol (10 mL) and oleic acid (20 mL) were mixed together to get a homogeneous solution. And the solid $Ln(NO_3)_3$ (0.6 mmol total amounts) dissolved in 1.2 mL ultrapure water was added. Then 1.0 M NaF (4 mL) aqueous

solution was added dropwise into the above mixture under extensive magnetic stirring. After agitating for another 10 min, the mixture was transferred to a 50 mL autoclave and hydrothermally treated at 160 ºC for 12 h. Afterwards the autoclave was cooled down to room-temperature naturally, and OA-modified UCPs were collected at the bottom of the container by cyclohexane, washed with cyclohexane/ethanol (1:6 v/v) for three times and centrifuged to obtain powder products.

2.4 Ligand-exchange of OA-modified UCPs into HDA-coated UCPs

The ligand-exchange process of OA-modified UCPs into HDA-coated UCPs was conducted according to a reported literature (Zhang et al., 2009). HDA (1.5 g) was added into 30 mL diethylene glycol (DEG) and the mixture was heated up to 110 ºC for 30 min with vigorous stirring under nitrogen. Then OA-modified UCPs (40 mg) dispersed in 2 mL of chloroform was injected into the above solution and heated to 240 ºC for 5 h. After the solution was naturally cooled down to room temperature, excess ultrapure water was added and HDA-coated UCPs were isolated and washed three times with ultrapure water by centrifugation. Finally they were dispersed in 4 mL of ultrapure water and stored at room temperature for use.

2.5 Preparation of MUDA modified PdNPs

The synthesis of MUDA modified PdNPs was accomplished through a one-step reduction method (Wang et al., 2012). Firstly, 2 mL NaOH with a concentration of 0.2 M was added into a 100 mL round-bottomed flask to dissolve 0.0066 g MUDA. Then 13 mL ultrapure water and 172 μL 85% $N_2H_4 \cdot H_2O$ was injected. Finally, 15 mL Na_2PdCl_4 (2 mM) was added dropwise into the above mixture in 1 h under extensive stirring. The color of the reaction mixture gradually turned into black accompanied with the addition of Na_2PdCl_4. After the agitation lasting for 30 min, the

MUDA modified PdNPs were separated by centrifugation and washed three times with ultrapure water. And the products were dispersed in 8 mL water with an ultimate concentration of 0.125 mg/mL.

2.6 Attachment of amine modified CEA Aptamer to HDA-coated UCPs

The standard EDC-NHS conjugation protocol was applied to covalently conjugate amine modified CEA aptamer to HDA-coated UCPs (Hermanson, 2008). Firstly, EDC·HCl with a concentration of 0.4 mM and NHS with a concentration of 1 mM were weighed and added into 2 mg of HDA-coated UCPs dispersed in 4 mL MES buffer (10 mM, pH 5.5) at the same time. The reaction was lasted for 45 min at room temperature to sufficiently activate the carboxyl groups of HDA on the surface of UCPs under gentle stirring. The carboxyl activated HDA-coated UCPs were centrifuged and washed with ultrapure water for three times. Then they were dispersed into 4 mL of HEPES buffer (10 mM, pH 7.2). And 2 nmol amino modified CEA aptamer was added into the above mixture followed by reacting overnight with slow shaking. Finally, 10 mg of Tris was added into the reaction mixture to block the excess NHS. The CEA aptamer attached UCPs were separated and washed three times with ultrapure water by centrifugation and diluted into 4 mL of Tris-HCl buffer (10 mM, pH 7.4). The concentration of the UCPs-CEA aptamer complex was 0.5 mg/mL (according to the concentration of UCPs) and it was stored at 4 ºC for further use.

2.7 CEA Detection in Aqueous Buffer Solution and Diluted Human Serum

To analyze the fluorescence quenching ability of MUDA modified PdNPs towards CEA aptamer attached UCPs, a fixed amount of UCPs-CEA aptamer complex (0.015 mg/mL) was incubated with increasing concentration of MUDA modified PdNPs in Tris-HCl buffer (10 mM, 50 mM NaCl, pH 7.4) at room temperature for 1 h, and then upconverting fluorescence spectra were

recorded. In order to do the upconverting fluorescence recovery experiments, different amounts of CEA were mixed with the UCPs-CEA aptamer complex (0.015 mg/mL) in Tris-HCl buffer (10 mM, 50 mM NaCl, pH 7.4) at room temperature for 2 h. Afterwards MUDA modified PdNPs with an ultimate concentration of 0.028 mg/mL were added one by one into the above mixtures followed by incubation for another 1 h at room temperature. Finally, the upconverting fluorescence intensity of the reaction mixture was recorded under the excitation wavelength of 980 nm. To examine the specificity of the FRET aptasensor towards CEA detection, IgE (5 μg/mL), BSA (600 μg/mL), glycine (100 pg/mL), glucose (100 pg/mL) and lysozyme (100 pg/mL) were added into the UCPs-CEA aptamer-PdNPs fluorescence quenching system respectively in place of CEA (100 pg/mL) followed by the same analytical procedures. In order to determine the applicability of this CEA biosensor in human serum matrix, fresh serum sample 100-fold diluted with Tris-HCl (10 mM, 50 mM NaCl, pH 7.4) was used as the assay medium and the assay procedure was the same as that in the aqueous solution. And standard addition method was also applied to detect the concentration of CEA in practical serum samples.

3. Results and discussion

3.1 Construction of the UC-FRET Biosensor for CEA

As reported by Li et al., there were strong coordination effect between PdNPs and heteroatom-containing biomolecules such as single-stranded DNA (ssDNA) and peptides (Li et al., 2015). However, after ssDNA hybridized with its complementary chain, the coordination effect was greatly weakened as less heteroatoms exposed to PdNPs in the double helix structure of DNA. Given this, the CEA biosensor based on the conformational change of CEA aptamer after interacting with CEA was proposed using UCPs as the FRET donor and PdNPs as the

FRET acceptor. The principle of the CEA biosensor was illustrated in Scheme 1, CEA aptamer attached UCPs were brought close to MUDA modified PdNPs in the range from 1 nm to 10 nm through the strong coordination interaction between CEA aptamer and PdNPs, which resulted in the FRET occurrence and the fluorescence quenching of UCPs was observed. Upon the introduction of CEA into the UCPs-CEA aptamer-PdNPs fluorescence quenching system, CEA aptamer preferentially bound to CEA accompanied by the conformational change, which largely weakened the coordination effect between CEA aptamer and PdNPs. Thus the distance between UCPs and PdNPs was widened and the FRET process was blocked. Therefore, the fluorescence recovery of UCPs was observed and the degree of fluorescence recovery was in a CEA concentration-dependent manner.

[Scheme 1]

3.2 Properties Characterization of the Fluorescence Donor

It has been reported that the surface plasmon resonance peak of small PdNPs (typically<10 nm in size) is located in the UV region (Creighton and Eadon, 1991) and they exihibit size-dependent SPR absorption properties (Xiong and Chen et al., 2005; Xiong and McLellan et al., 2005; Zhang et al., 2013). Li et al. have synthesized 31 nm PdNPs and found that its strong light absorption covered nearly the whole ultraviolet-visible range (Li et al., 2015). In order to ensure the occurrence of FRET process, the fluorescence spectrum of energy donor need to be effectively overlapped with the absorption spectrum of energy acceptor. $NaYF_4$:Yb, Tm nanoparticles which fluoresce strongly at 480 nm were used as the energy donor in this FRET biosensor. Firstly OA modified $NaYF_4$:Yb,Tm nanoparticles were prepared through a solvothermal synthesis method. Then a ligand-exchange process was applied to obtain water-dispersible HDA-coated UCPs,

which is similar to that in our previous work (Li et al., 2014). The weaker peak at ν=3004 cm^{-1}, attributable to the =C−H stretching vibration in the FT-IR spectrum of HDA-coated UCPs compared with that of the OA-modified UCPs, firmly indicates the successful ligand-exchange process (Fig. 1f). As shown in the TEM image (Fig. 1a and 1b), the OA-modified UCPs and HDA-coated UCPs both show good dispersion property with the diameter ranging from 10 nm to 20 nm. The high-resolution TEM images display clear lattice fringes for the OA-modified UCPs and HDA-coated UCPs, which verifies the high crystallinity of the UCPs. The X-ray diffraction (XRD) pattern indicated that the synthesized OA-modified UCPs and HDA-coated UCPs were mainly in cubic phase (Fig. 1d and 1e).

[Fig.1]

3.3 Properties Characterization of the Energy Acceptor

In consideration of the negatively charged nature of HDA-coated UCPs, MUDA modified PdNPs were used in this biosensor to avoid the side effect caused by electrostatic attraction. PdNPs were synthesized using Na_2PdCl_4 as the precursor and $N_2H_4 \cdot H_2O$ as the reducing agent in the presence of MUDA as the capping agent (Wang et al., 2012). It is indicated in Fig. 2a that the MUDA modified PdNPs are nearly round in shape with an average diameter of 16 nm. The XRD pattern revealed a face-centered cubic (fcc) Pd crystal structure (JCPDS card, 05-0681) of the 16 nm MUDA modified PdNPs (Fig. 2b). The existence of MUDA on the surface of PdNPs was verified by FT-IR measurement (Fig. 2c). The peaks at ν = 2850 cm^{-1} and ν = 2920 cm^{-1} are attributable to the presence of methylene group. And the appearance of the peak at 1632 cm^{-1} confirmed the presence of –COOH groups on MUDA modified PdNPs (Wang et al., 2012). The UV-vis absorption spectrum of MUDA modified PdNPs in Fig. 2d clearly showed that it

exhibited strong absorption in nearly the whole UV-vis spectral range. So it can be safely inferred that MUDA modified PdNPs has the potential to be effective fluorescence quencher for HDA modified UCPs (emission at 480 nm).

[Fig. 2]

3.4 Construction of the UC-FRET Biosensor

As designed in Scheme 1, amine modified CEA aptamer was attached to HDA-coated UCPs through standard EDC-NHS conjugation protocol. The appearance of a new absorption peak at 260 nm in the UV-vis absorption spectrum of HDA-coated UCPs after conjugation with CEA aptamer firmly indicated that CEA aptamer attached UCPs were obtained (Fig. 3a). It has been calculated that 0.83 nmol CEA aptamer was attached to 1 mg HDA modified UCPs by subtracting the amount of CEA aptamer in the supernatant from the total CEA aptamer added in the labeling procedure. The TEM image of CEA aptamer modified UCPs was shown in Fig. 1c. In the FT-IR spectrum of CEA aptamer modified UCPs (Fig. 1f), the new peak appeared at 1260 cm^{-1} was ascribed to the C-N stretching vibration. In order to examine the fluorescence quenching ability of PdNPs towards UCPs, an increasing concentration of MUDA modified PdNPs were added into a fixed amount of CEA aptamer attached UCPs (0.015 mg/mL). After incubation for a short while, a PdNPs concentration-dependent fluorescence quenching phenomenon of CEA aptamer attached UCPs was observed with the maximum quenching efficiency reaching 85% in the presence of 0.028 mg/mL MUDA modified UCPs (Fig. 3b). It was ascribed to the strong coordination effect between heteroatom-containing CEA aptamer and PdNPs which brought UCPs in close to PdNPs and FRET occurred. As the phosphoric acid skeleton of the CEA aptamer and MUDA modified PdNPs were both negatively charged,

electrostatic attraction could be effectively excluded to be the reason for FRET occurrence. In addition, after mixing a concentration of 0.015 mg/mL HDA-coated UCPs with MUDA modified PdNPs (0.028 mg/mL) in Tris-HCl buffer, the fluorescence intensity of HDA-coated UCPs was nearly unchanged (Fig. 3c). So the non-specific fluorescence quenching caused by PdNPs towards UCPs could also be eliminated. The time dependence of fluorescence quenching efficiency (Fig. 3d) indicated that it only took 35 min to reach the quenching equilibrium. In the following fluorescence recovery experiments, In order to ensure reaching the quenching equilibrium and getting stable fluroescence signal, 1 h incubation time was chosen for the fluorescence quenching experiment.

[Fig. 3]

3.5 CEA Detection in Aqueous Buffer Solution

After introduction of CEA into the UCPs-CEA aptamer-PdNPs FRET quenching system in the Tris-HCl buffer, CEA aptamer preferentially bound to CEA accompanied by the conformational change of CEA aptamer, which greatly weakened the coordination effect between CEA aptamer and PdNPs. Therefore the FRET process was inhibited and fluorescence recovery of UCPs was observed accordingly. As indicated in Fig. 4a, the degree of fluorescence recovery was in a CEA concentration-dependent manner. A linear relationship between the fluorescence recovery of UCPs and the concentration of CEA in the range from 2 pg/mL to 100 pg/mL was obtained in the Tris-HCl buffer, with the detection limit of 0.8 pg/mL (calculated as the concentration corresponding to three times of the standard deviation of the background signal from seven independent measurements) (Fig. 4b). Lin et al. have developed a CEA fluorescence biosensor based on the FRET between polymer dots and Au nanoparticles in the range of 0.1-10 ng/mL (Lin

et al., 2014). It has also been reported that CEA detection based on FRET between quantum dots and graphene oxide was realized in the range from 0.257 to 12.9 ng/mL (Zhou et al., 2014). Compared to the previously reported FRET biosensors for CEA detection, the sensitivity of the present sensor is greatly improved, which shows great potential to detect lower concentration of CEA in practical samples. The significant performance improvement of this FRET biosensor was largely relied on the excellent fluorescence quenching ability of PdNPs towards UCPs with almost negligible non-specific fluorescence quenching, which is a great advantage of PdNPs as energy acceptor in FRET biosensors compared to other FRET acceptors, such as organic dyes or carbon-based nanomaterials. Interfering substances including IgE, BSA, glycine, glucose and lysozyme were individually added into the above UCPs-CEA aptamer-PdNPs FRET system in place of CEA to examine the specificity of this FRET biosensor for CEA in Tris-HCl buffer. And the experimental procedures were all the same as that for CEA detection. As can be seen from Fig. 4c, interference substances all cause negligible fluorescence variation of UCPs compared to CEA. The result firmly indicated that this FRET biosensor exhibited excellent specifity towards CEA, in which the highly specific affinity between CEA aptamer and CEA took an important role.

[Fig. 4]

3.6 CEA Detection in Human Serum Sample

Monitoring the serum concentration of CEA is very important in the process of clinical diagnosis and prognosis of tumor. UCPs which are excited by near infrared (NIR) light and emit fluorescence in the visible range, can effectively overcome the adverse effect of background fluorescence and scattering light on the detection sensitivity caused by complex serum matrix under UV-vis illumination in optical sensing. FRET biosensors based on UCPs as the energy

donor have been widely used for biomolecules detection in serum samples (Rantanen et al., 2008; Wang et al., 2013; Li et al., 2014). In this paper, CEA detection was also realized in 100-fold diluted human serum sample with Tris-HCl buffer (10 mM, 50 mM, pH 7.4) by view of the advantage of UCPs under the same experimental procedures as that in the aqueous buffer solution. It can be seen from Fig. 5a that the fluorescence of UCPs was recovered in a CEA concentration-dependent manner. And the degree of fluorescence restoration was linear related to the concentration of CEA in the range from 4 pg/mL to 100 pg/mL, with a detection limit of 1.7 pg/mL (calculated as the concentration corresponding to three times of the standard deviation of the background signal from seven independent measurements) (Fig. 5b). The narrower linear range and higher detection limit may be ascribed to the complexity of the serum sample. Standard addition experiments were conducted to examine the feasibility of this CEA biosensor in practical serum samples. The initial CEA values in the diluted serum samples were measured with a low relative standard deviation (RSD) between 1.0 and 3.0, demonstrating the high reproducibility of this CEA biosensor. the satisfactory recoveries from 93% to 103% in Table 1 convincingly demonstrates that this FRET biosensor based on the efficient fluorescence resonance energy transfer between UCPs and PdNPs has great potential in practical application.

[Fig. 5]

[Table 1]

4. Conclusions

In summary, an ultrasensitive FRET biosensor for CEA detection has been constructed based on the efficient fluorescence quenching ability of PdNPs towards UCPs with negligible non-specific fluorescence quenching. The application of NIR-excited UCPs and CEA aptamer

with high affinity and specificity also contributes to the good performance of this biosensor in both aqueous buffer solution and human serum samples. In consideration of its simple configuration and operation, the homogeneous FRET biosensor can be widely used to detect a variety of biomolecules in future.

Acknowledgements

The authors acknowledge the financial support from the National Natural Science Foundation of China (No. 21375098).

References

Achatz, D.-C.D.E., Meier, D.-C.R.J., Fischer, D.-C.L.H., Wolfbeis, O.S., 2011. Angew. Chem. Int. Ed. 50, 260-263.

Bogdan, N., Vetrone, F., Roy, R., Capobianco, J.A., 2010. J. Mater. Chem. 20, 7543-7550.

Creighton, J.A., Eadon, D.G., 1991. J. Chem. Soc., Faraday Trans. 87, 3881-3891.

Cui, S.S., Chen, H.Y., Gu, Y.Q., 2011. J. Phys. Conference Series 277, 012006.

EI-Masry, S., EI-Sayed, I.H., Lotfy, M., Mahmoud, L., EI-Naggar, M., 2007. J. Immunoass. Immunoch. 28, 91-105.

Hashemi Tabar, G.R., Smith, C.L., 2010. World Appl. Sci. J. 8, 16-21.

Hermanson, G.T., 2008. Bioconjugate Techniques, second ed. Academic, San Diego.

Kandela, I.K., Bleher, R., Albrecht, R.M., 2007. J. Histochem. Cytochem. 55, 983-990.

Kim, J., Kwon, S., Park, J.-K., Park, I., 2014. Biosens. Bioelectron. 55, 209-215.

Kuningas, K., Rantanen, T., Ukonaho, T., Lövgren, T., Soukka, T., 2005. Anal. Chem. 77, 7348-7355.

Kuningas, K., Ukonaho, T., Päkkilä, H., Rantanen, T., Rosenberg, J., Lövgren, T., Soukka, T., 2006. Anal. Chem. 78, 4690-4696.

Laboria, N., Fragoso, A., Kemmner, W., Latta, D., Nilsson, O., Botero, M.L., Drese, K., O'Sullivan, C.K., 2010. Anal. Chem. 82, 1712-1719.

Ladd, J., Lu, H., Taylor, A.D., Goodell, V., Disis, M.L., Jiang, S., 2009. Colloid. Surface. B 70, 1-6.

Lee, J.U., Nguyen, A.H., Sim, S.J., 2015. Biosens. Bioelectron. 74, 341-346.

Li, H., Sun, D.E., Liu, Y.J., Liu, Z.H., 2014. Biosens. Bioelectron. 55, 149-156.

Li, H., Sun, D.E., Liu, Z.H., 2015. Chem. Eur. J. 21, 4944-4948.

Lin, Z.Y., Zhang, G.Y., Yang, W.Q., Qiu, B., Chen, G.N., 2012. Chem. Commun. 48, 9918-9920.

Liu, W., Yang, H., Ding, Y., Ge, S., Yu, J., Yan, M., Song, X., 2014. Analyst 139, 251-258.

Liu, S., Zhang, L., Yang, T., Yang, H., Zhang, K.Y., Zhao, X., Lv, W., Yu, Q., Zhang, X., Zhao, Q., Liu, X., Huang, W., 2014. ACS Appl. Mater. Interfaces 6, 11013-11017.

Luo, C., Wen, W., Lin, F., Zhang, X., Gu, H., Wang, S., 2015. RSC Adv. 5, 10994-10999.

Lv, W., Yang, T., Yu, Q., Zhao, Q., Zhang, K.Y., Liang, H., Liu, S., Li, F., Huang, W., 2015. Adv. Sci. 2, 1500107.

Ma, T., Ma, Y., Liu, S., Zhang, L., Yang, T., Yang, H.R., Lv, W., Yu, Q., Xu, W., Zhao, Q., Huang, W. 2015. J. Mater. Chem. C 3, 6616-6620.

Martínez-Mancera, F.D., García-López, P., Hernández-López, J.L., 2015. Clin. Chim. Acta 444, 199-205.

Meyer, D.A., Oliver, J.A., Albrecht, R.M., 2010. Microsc. Microanal. 16, 33-42.

Pal, S., Bhand, S., 2015. Microchim. Acta 182, 1643-1651.

Qu, S., Liu, J., Luo, J., Huang, Y., Shi, W., Wang, B., Cai, X., 2013. Clin. Chim. Acta 766, 94-99.

Rantanen, T., Järvenpää, M.-L., Vuojola, J., Kuningas, K., Soukka, T., 2008. Angew. Chem. Int. Ed. 120, 3871-3873.

Song, K., Kong, X.G., Liu, X.M., Zhang, Y.L., Zeng, Q.H., Tu, L.P., Shi, Z., Zhang, H., 2012. Chem. Commun. 48, 1156-1158.

Špringer, T., Ermini, M.L., Špačková, B., Jabloňků, J., Homola, J., 2014. Anal. Chem. 86, 10350-10356.

Urva, S.R., Yang, V.C., Balthasar, J.P., 2009. J. Immunoass. Immunoch. 30, 418-427.

Wang, D.F., Li, Y.Y., Lin, Z.Y., Qiu, B., Guo, L.H., 2015. Anal. Chem. 87, 5966-5972.

Wang, L.Y., Yan, R.X., Huo, Z.Y., Wang, L., Zeng, J.H., Bao, J., Wang, X., Peng, Q., Li, Y.D., 2005, Angew. Chem. Int. Ed. 44, 6054-6057.

Wang, M., Hou, W., Mi, C.C., Wang, W.X., Xu, Z.R., Teng, H.H., Mao, C.B., Xu, S.K., 2009, Anal. Chem. 81, 8783-8789.

Wang, Y.H., Bao, L., Liu, Z.H., Pang, D.W., 2011. Anal. Chem. 83, 8130-8137.

Wang, Y.H., Wu, Z.J., Liu, Z.H., 2013. Anal. Chem. 85, 258-264.

Wang, Z.F., Li, H.Y., Zhen, S., He, N.Y., 2012. Nanoscale 4, 3536-3542.

Wu, K., Chu, C., Ma, C., Yang, H., Yan, M., Ge, S., Yu, J., Song, X., 2015. Sens. Actuators B: Chem. 206, 43-49.

Wu, S.J., Duan, N., Ma, X.Y., Xia, Y., Wang, H.X., Wang, Z.P., Zhang, Q., 2012. Anal. Chem. 84, 6263-6270.

Xiao, Y., Zeng, L.Y., Xia, T., Wu, Z.J., Liu, Z.H., 2015. Angew. Chem. Int. Ed. 54, 5323-5327.

Xiong, Y., Chen, J., Wiley, B., Xia, Y., Yin, Y., Li, Z.-Y., 2005. Nano Lett. 5, 1237-1242.

Xiong, Y., McLellan, J.M., Chen, J., Yin, Y., Li, Z.Y., Xia, Y. 2005, J. Am. Chem. Soc. 127, 17118-17127.

Yang, X.M., Zhuo, Y., Zhu, S.S., Luo, Y.W., Feng, Y.J., Xu, Y., 2015. Biosens. Bioelectron. 64, 345-351.

Zeng, L.Y., Yuan, Y.X., Shen, P., Wong, K.-Y., Liu, Z.H., 2013. Chem. Eur. J. 19, 8063-8067.

Zeng, X.X., Ma, S.S., Bao, J.C., Tu, W.W., Dai, Z.H., 2013. Anal. Chem. 85, 11720-11724.

Zhang, C.L., Yuan, Y.X., Zhang, S.M., Wang, Y.H., Liu, Z.H. 2011. Angew. Chem. Int. Ed. 50, 6851-6854.

Zhang, H., Jin, M., Xiong, Y., Lim, B., Xia, Y., 2013. Acc. Chem. Res. 46, 1783-1794.

Zhang, Q.B., Song, K., Zhao, J.W., Kong, X.G., Sun, Y.J., Liu, X.M., Zhang, Y.L., Zeng, Q.H., Zhang, H., 2009. J. Colloid Interface Sci. 336, 171-175.

Zhou, Z.-M., Feng, Z., Zhou, J., Fang, B.-Y., Qi, X.-X., Ma, Z.-Y., Liu, B. Zhao, Y.-D., Hu, X.-B., 2015. Biosens. Bioelectron. 64, 493-498.

Zhou, Z.-M., Zhou, J., Chen, J., Yu, R.N., Zhang, M.Z., Song, J.T., Zhao, Y.D., 2014. Biosens. Bioelectron. 59, 397-403.

Figures and Tables Captions

Scheme 1. Schematic Illustration of the CEA Biosensor Based on FRET from CEA Aptamer-Attached UCPs to PdNPs.

Fig. 1 (a) TEM image of OA-modified UCPs, the inset was the HR-TEM of the OA-modified UCPs. (b) TEM image of HDA-coated UCPs, the inset was the HR-TEM image of HDA-coated UCPs. (c) TEM image of CEA aptamer-attached UCPs. (d) XRD pattern of OA-modified

△ △

UCPs: , cubic phase (JCPDS file no. 77-2042). (e) XRD pattern of HDA-coated UCPs: , cubic phase (JCPDS file no. 77-2042). (f) FT-IR spectra of OA-modified UCPs, HDA-coated UCPs and CEA aptamer-attached UCPs.

Fig. 2 (a) TEM image of the MUDA modified PdNPs. (b) XRD pattern of MUDA modified PdNPs. (c) FT-IR spectrum of the MUDA modified PdNPs. (d) UV-vis absorption spectrum of MUDA modified PdNPs.

Fig. 3 (a) UV-vis absorption spectra of HDA modified UCPs and CEA aptamer attached UCPs (0.5 mg/mL). (b) Fluorescence quenching of CEA aptamer attached UCPs after introduction of different concentrations of MUDA-modified PdNPs (0, 0.009 mg/mL, 0.019 mg/mL, 0.028 mg/mL, 0.038 mg/mL, 0.047 mg/mL). (c) Fluorescence quenching of HDA modified UCPs in the presence of 0.028 mg/mL MUDA modified PdNPs. (d) Time dependence of the fluorescence quenching degree for 0.015 mg/mL CEA aptamer attached UCPs caused by 0.028 mg/mL MUDA modified PdNPs. All experiments were performed in Tris-HCl buffer (10 mM, 50 mM NaCl, pH 7.4) under excitation at 980 nm.

Fig. 4 (a) Fluorescence recovery of the biosensor with the addition of increasing concentration of CEA (0, 2 pg/mL, 8 pg/mL, 20 pg/mL, 40 pg/mL, 80 pg/mL, 100 pg/mL). (b) The linear relationship between the fluorescence recovery degree (at 480 nm) and the concentration of CEA within the range from 2-100 pg/mL, data were presented as average ±SD from three independent measurements. (c) Relative fluorescence intensity ((F/F_0)) of the UCPs-CEA aptamer-PdNPs FRET biosensor in the presence of CEA and other molecules individually, where F_0 is the fluorescence intensity of the UCPs-CEA aptamer-PdNPs fluorescence quenching system in the absence of CEA or other molecules and F is the fluorescence intensity of the UCPs-CEA

aptamer-PdNPs fuorescence quenching system in the presence of CEA or other molecules. Data were presented as average ±SD from three independent measurements. The concentration of IgE was 5 μg/mL, the concentration of BSA was 600 μg/mL, the concentration of CEA, glycine, glucose and lysozyme were all 100 pg/mL. Experiments were conducted in Tris-HCl buffer (10 mM, 50 mM NaCl, pH 7.4) with 0.015 mg/mL CEA aptamer attached UCPs and 0.028 mg/mL MUDA modified PdNPs under excitation at 980 nm.

Fig. 5 (a) Fluorescence spectra of the biosensor with the introduction of different amounts of CEA (0, 4 pg/mL, 8 pg/mL, 20 pg/mL, 40 pg/mL, 60 pg/mL, 100 pg/mL) in human serum 100-fold diluted with Tris-HCl buffer (10 mM, 50 mM NaCl, pH 7.4). (b) The linear relationship between the fluorescence recovery degree (at 480 nm) and the concentration of CEA within the range from 4 pg/mL to 100 pg/mL, data were presented as average ±SD from three independent measurements. All experiments were performed in the presence of 0.015 mg/mL CEA aptamer attached UCPs and 0.028 mg/mL MUDA modified PdNPs under excitation at 980 nm.

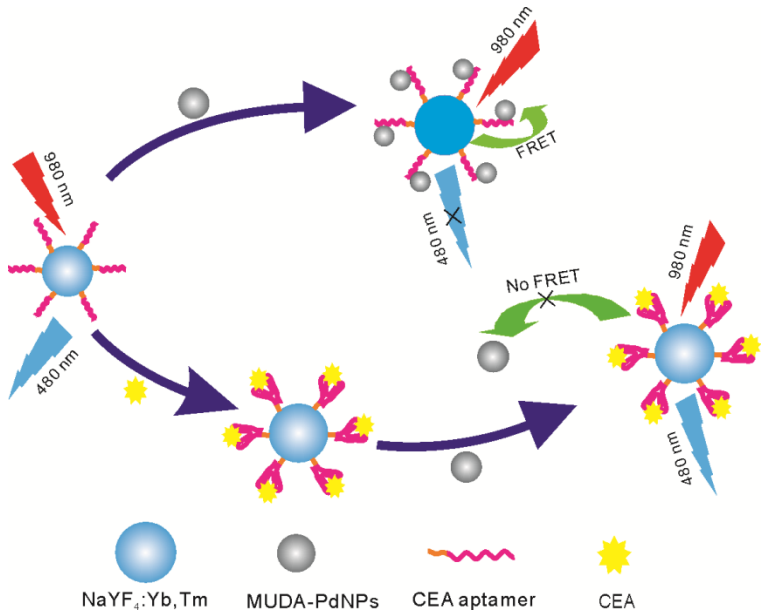

Scheme. 1

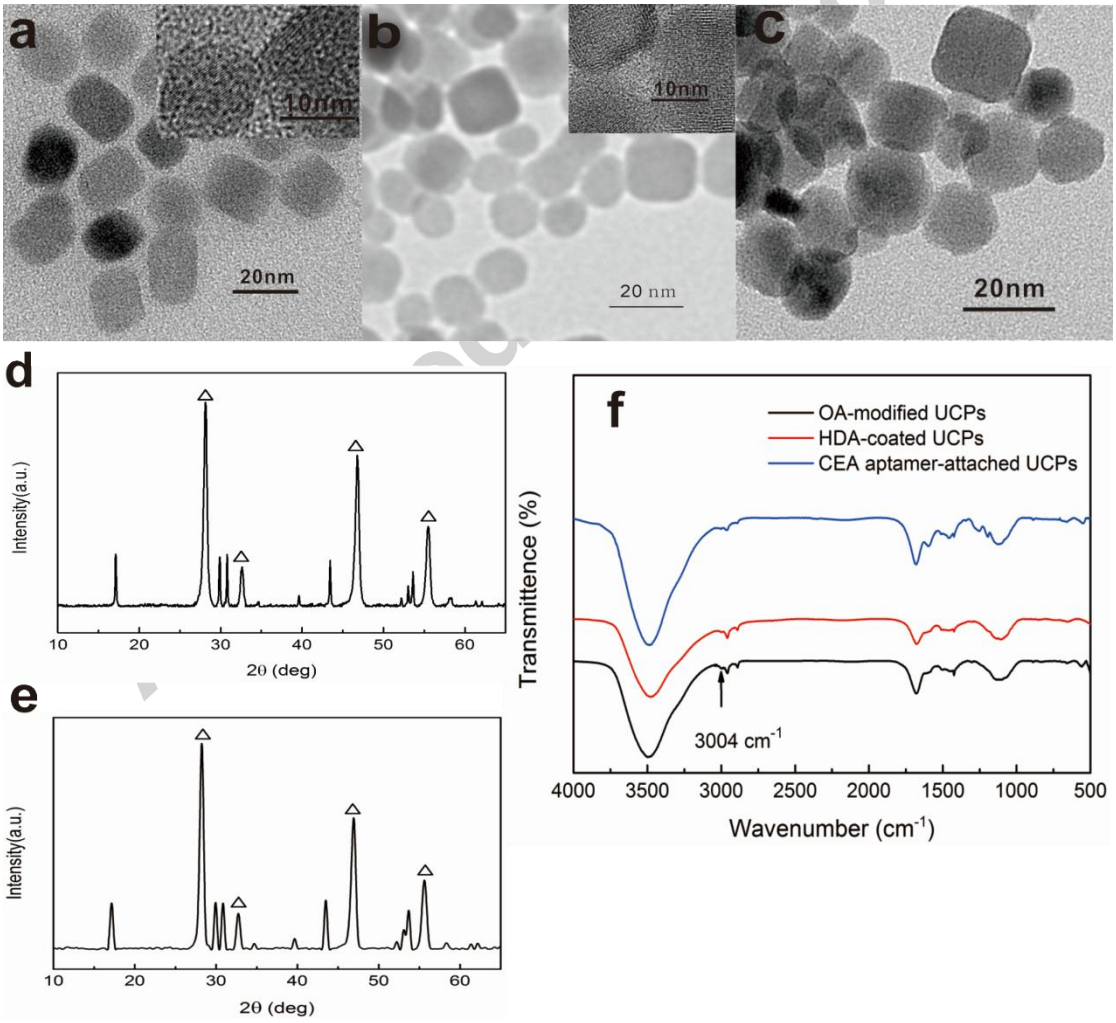

Fig. 1

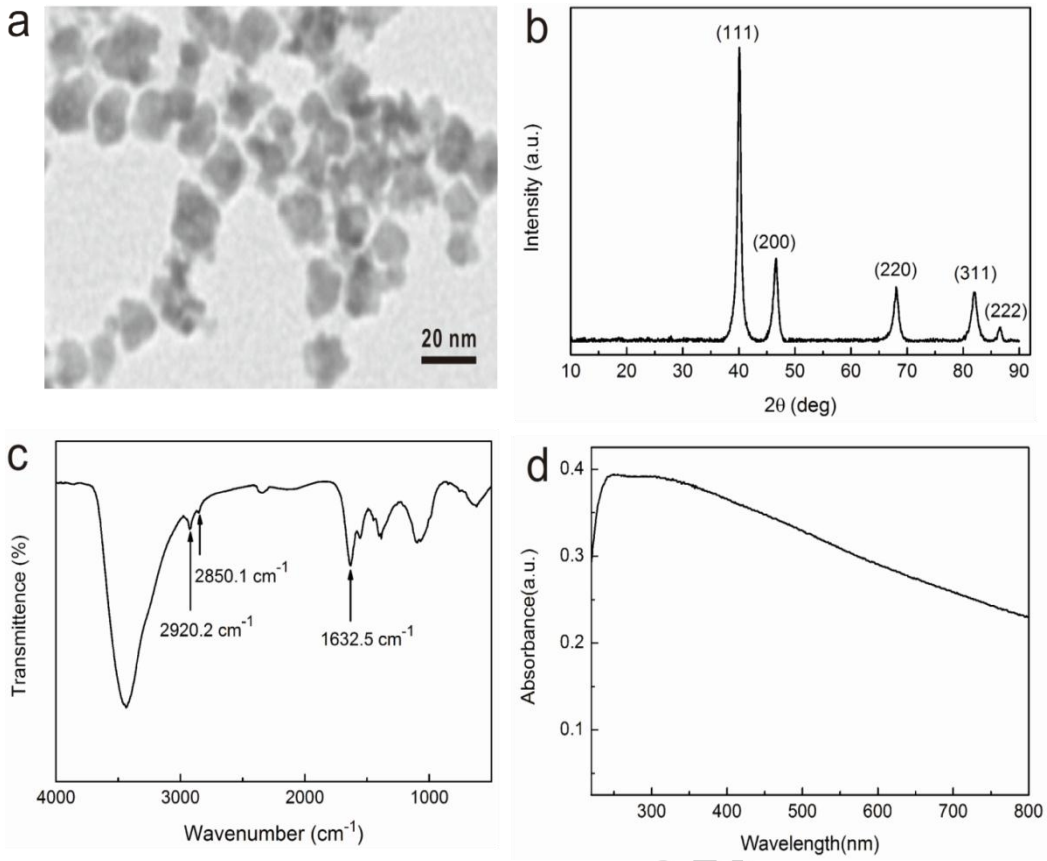
a
20 nm
b
(111)
(200)
(220)
(311)
(222)
Intensity (a.u.)
2θ (deg)
c
Transmittence (%)
2850.1 cm-1
2920.2 cm-1
1632.5 cm-1
Wavenumber (cm-1)
d
Absorbance(a.u.)
Wavelength(nm)

Fig. 2

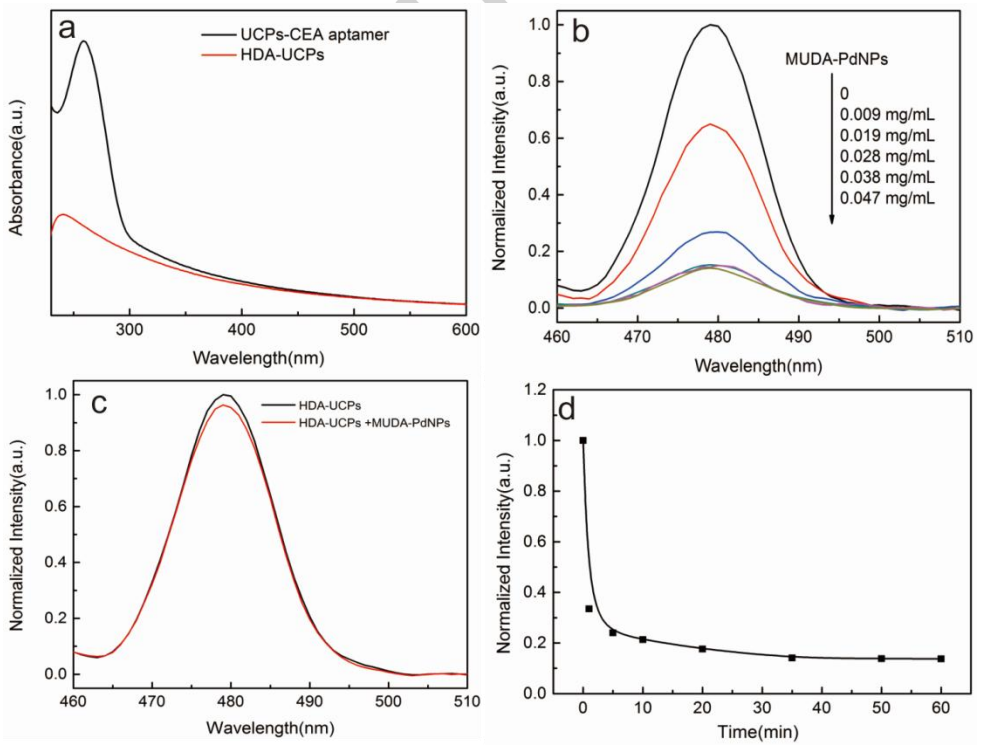
a
UCPs-CEA aptamer
HDA-UCPs
Absorbance(a.u.)
Wavelength(nm)
b
MUDA-PdNPs
0
0.009 mg/mL
0.019 mg/mL
0.028 mg/mL
0.038 mg/mL
0.047 mg/mL
Normalized Intensity(a.u.)
Wavelength(nm)
c
HDA-UCPs
HDA-UCPs +MUDA-PdNPs
Normalized Intensity(a.u.)
Wavelength(nm)
d
Normalized Intensity(a.u.)
Time(min)

Fig. 3

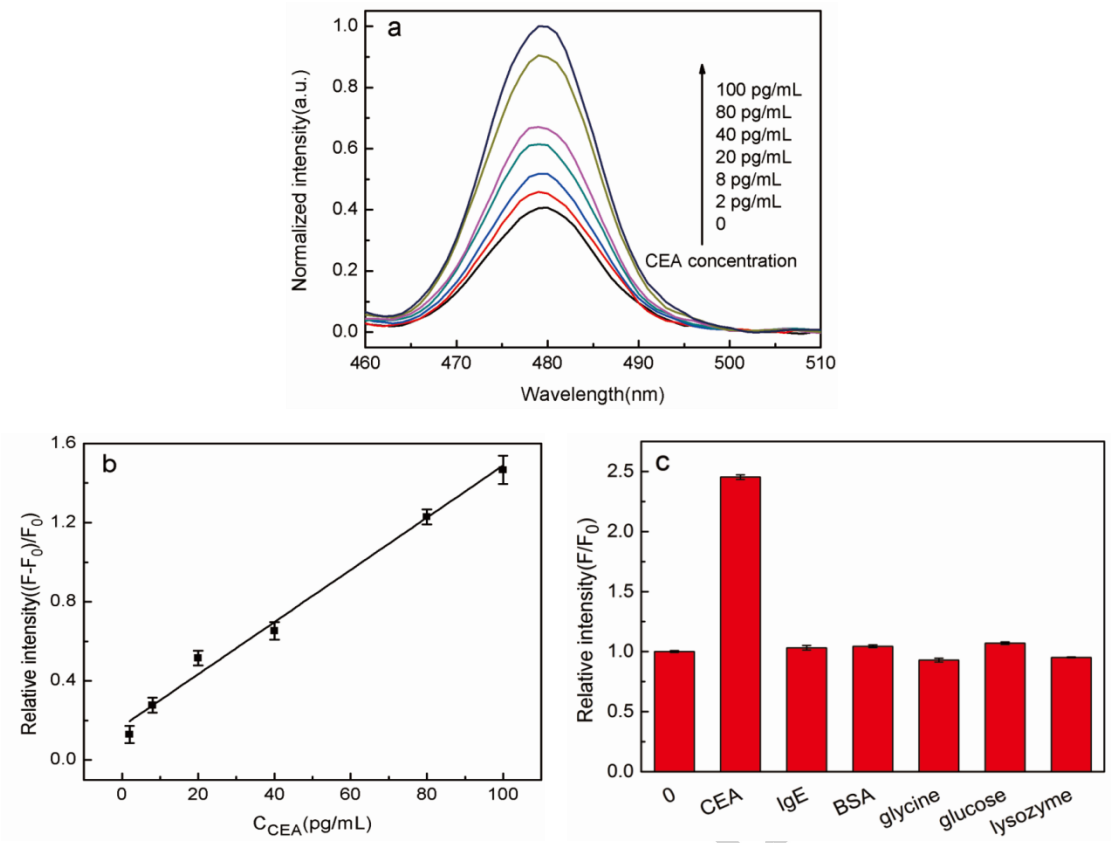
a
Normalized intensity(a.u.)
Wavelength(nm)
100 pg/mL
80 pg/mL
40 pg/mL
20 pg/mL
8 pg/mL
2 pg/mL
0
CEA concentration
b
Relative intensity((F-F0)/F0)
CCEA(pg/mL)
c
Relative intensity(F/F0)
0
CEA
IgE
BSA
glycine
glucose
lysozyme

Fig. 4

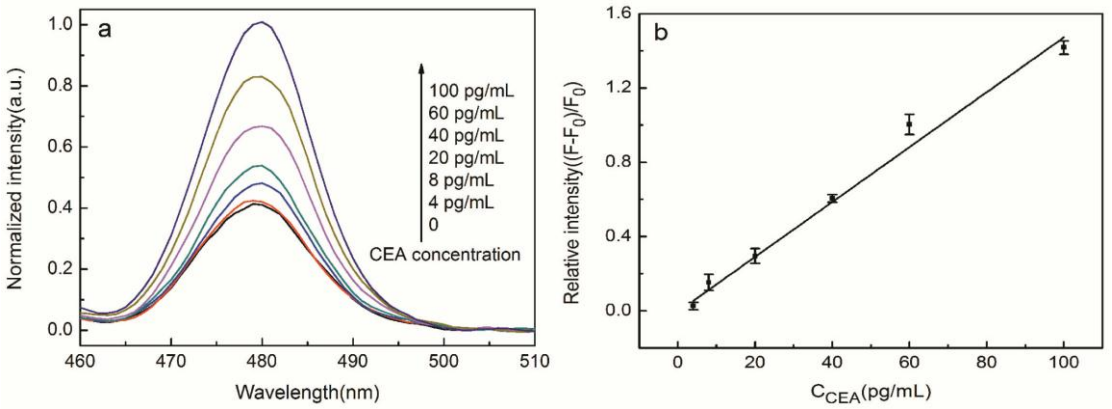
a
Normalized intensity(a.u.)
Wavelength(nm)
100 pg/mL
60 pg/mL
40 pg/mL
20 pg/mL
8 pg/mL
4 pg/mL
0
CEA concentration
b
Relative intensity((F-F0)/F0)
CCEA(pg/mL)

Fig. 5

Table. 1 Determination of CEA in three real serum samples.

Sample No	Measured (pg/mL)[a]	RSD (%) n=3	Added (pg/mL)	Found (pg/mL)[a]	Recovery (%)	RSD (%) n=3
1	19.45	2.3	6	25.65	103	3.9
2	32.45	1.0	5	37.09	93	1.4
3	12	3.0	6	17.68	95	1.5

[a]Mean value of three determinations by the biosensor.

Highlights

- A FRET biosensor for CEA detection was constructed based on upconverting nanoparticles as the energy donor and palladium nanoparticles as the energy acceptor.
- Palladium nanoparticles exhibited excellent fluorescence quenching ability towards upconverting nanoparticles.
- The conformation change of CEA aptamer after interaction with the target caused the fluorescence recovery of upconverting nanoparticles.
- This CEA biosensor performs well in both aqueous buffer solution and human serum samples.
- This FRET biosensor has broad application prospects in detecting a variety of biomolecules in future.